CDF/DOC/BOTTOM/PUBLIC/10244
Draft 1.1
August 11, 2010

Observation of a Narrow Near-Threshold Structure in the $J/\psi\phi$ Mass Spectrum in $B^+ \to J/\psi\phi K^+$ Decays

The CDF Collaboration

(Dated: August 11, 2010)

Observation is reported for a structure near the $J/\psi\phi$ threshold, in $B^+ \to J/\psi\phi K^+$ decays produced in $\bar{p}p$ collisions at $\sqrt{s} = 1.96$ TeV with a statistical significance of beyond 5 standard deviations. There are 19 ± 6 events observed for this structure at a mass of $4143.4^{+2.9}_{-3.0}$(stat) $\pm$ 0.6(syst) MeV/c^2 and a width of $15.3^{+10.4}_{-6.1}$(stat) $\pm$ 2.5(syst) MeV/c^2, which are consistent with the previous measurements reported as evidence of the $Y(4140)$.

PACS numbers: 14.40.Gx, 13.25.Gv, 12.39.Mk

The existence of exotic mesons beyond $q\bar{q}$ has been discussed for many years [1], but evidence for such mesons has not been clearly established. The recently discovered states that have charmonium-like decay modes [2–5] but are difficult to place in the overall charmonium system have introduced challenges to conventional $q\bar{q}$ meson model. The possible interpretations beyond $q\bar{q}$ such as hybrid ($q\bar{q}g$) and four-quark states ($q\bar{q}q\bar{q}$) have revitalized interest in exotic mesons in the charm sector [6–11].

Recently, evidence has been reported by CDF for a narrow structure near the $J/\psi\phi$ threshold named as $Y(4140)$ in $B^+ \to J/\psi\phi K^+$ decays produced in $\bar{p}p$ collisions at $\sqrt{s} = 1.96$ TeV [12]. The structure is the first charmonium-like structure decaying into two heavy quarkonium states($c\bar{c}$ and $s\bar{s}$) which is accessible to exotic mesons such as a four-quark state, hybrid and glueball [7, 11, 13]. Since the mass of $Y(4140)$ is well beyond the threshold of open charm pair production, the expected branching fraction into this channel for conventional charmonium is tiny. Some interpretations beyond $q\bar{q}$ of the $Y(4140)$ have been proposed[14]. It is important to confirm the $Y(4140)$ [12] and investigate more potential structures in the $J/\psi\phi$ mass spectrum using data collected with the CDF II detector.

In this note, we report an update on a search for structures in the $J/\psi\phi$ system produced in exclusive $B^+ \to J/\psi\phi K^+$ decays with $J/\psi \to \mu^+\mu^-$ and $\phi \to K^+K^-$. This analysis is based on a sample of $\bar{p}p$ collision data at $\sqrt{s} = 1.96$ TeV with an integrated luminosity of about 6.0 fb^{-1} collected by the CDF II detector at the Tevatron. An update by using the same requirements applied in the previous analysis is described in this note.

The CDF II detector has been described in detail elsewhere [15]. The important components for this analysis include the tracking, muon, and time-of-flight (TOF) systems. The tracking system is composed of a silicon-strip vertex detector (SVX) surrounded by an open-cell drift chamber system called the central outer tracker (COT) located inside a solenoid with a 1.4 T magnetic field. The COT and SVX are used for the measurement of charged-particle trajectories and vertex positions. In addition, the COT provides ionization energy loss information, dE/dx, used for particle identification (PID), while the TOF system provides complementary PID information. The muon system is located radially outside the electromagnetic and hadronic calorimeters and consists of two sets of drift chambers and scintillation counters. The central part covers the pseudorapidity region $|\eta| \leq 0.6$ and detects muons with $p_T \geq 1.4$ GeV/c [16], and the second part covers the region $0.6 < |\eta| < 1.0$ and detects muons with $p_T \geq 2.0$ GeV/c.

In this analysis, $J/\psi \to \mu^+\mu^-$ events are recorded using a dedicated three-level dimuon trigger. The first trigger level requires two muon candidates with matching tracks in the COT and muon systems. The second level applies additional kinematic requirements to the muon pair candidate. The third level requires the invariant mass of the $\mu^+\mu^-$ pair to be within the range of 2.7 to 4.0 GeV/c^2. This dimuon trigger is prescaled at high instantaneous luminosity, so events from a slightly different dimuon trigger used by some CDF analyses [17] are included to increase statistics.

The invariant mass of $J/\psi\phi K^+$ after applying the same requirements used in the previous analysis [12] is shown in Fig. 1. A fit with a Gaussian signal function with its rms fixed to the value 5.9 MeV/c^2 obtained from Monte Carlo (MC) simulation [21] and a linear background function to the mass spectrum of $J/\psi\phi K^+$ returns a B^+ signal of 115 ± 12(stat) events. We increased the $B^+ \to J/\psi\phi K^+$ statistics by 53% comparing to previous analysis [12]. We then select B^+ signal candidates with a mass within 3σ (17.7 MeV/c^2) of the nominal B^+ mass as before. We define those events with a mass within [-9,-6]σ or [6,9]σ of nominal B mass as B sideband events; they are already

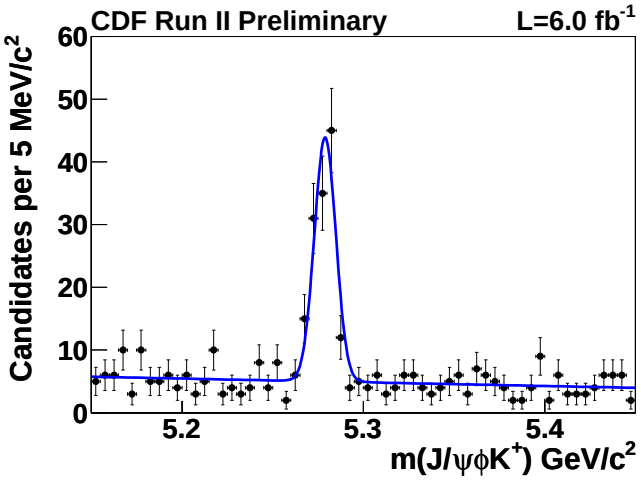

FIG. 1: The mass distribution of $J/\psi\phi K^+$; the solid line is a fit to the data with a Gaussian signal function and linear background function.

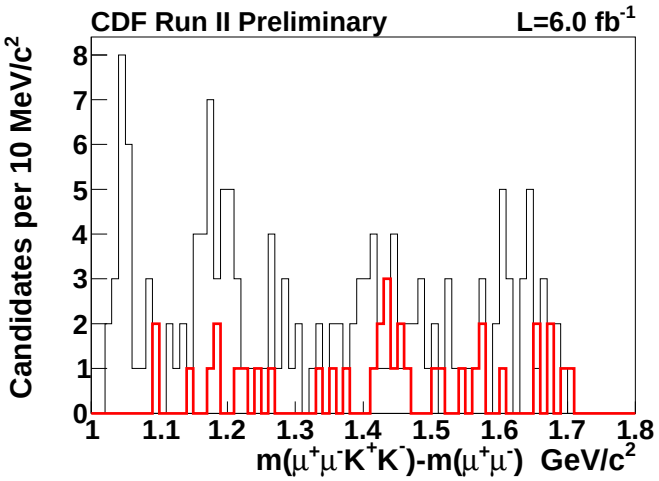

FIG. 2: The mass difference, ΔM, between $\mu^+\mu^-K^+K^-$ and $\mu^+\mu^-$, in the B^+ mass window is shown as the black histogram. The red histogram is the ΔM distribution from the data in the B sideband.

normalized to the B signal region assuming a linear background distribution. Fig. 2 shows the mass difference, $\Delta M = m(\mu^+\mu^-K^+K^-) - m(\mu^+\mu^-)$, for events in the B^+ mass window as well as in the B sideband in our data sample. Again we exclude masses above 1.56 GeV/c^2 to avoid backgrounds that are expected from misidentified $B_s^0 \to \psi(2S)\phi \to (J/\psi\pi^+\pi^-)\phi$ decays [12]. Figure 3 shows the Dalitz plot of $m^2(\phi K^+)$ versus $m^2(J/\psi\phi)$ for events in the B^+ mass window in our data sample. The comparison of the ΔM distribution in the B mass window for the dataset used in this analysis (6.0 fb^{-1}) and the dataset used in the previous analysis (2.7 fb^{-1} [12]) is shown in Figure 4.

The same model is used to examine the $Y(4140)$ structure as described in reference [12]. We model the enhancement by an S-wave relativistic BW function [22] convoluted with a Gaussian resolution function with the r.m.s. fixed to 1.7 MeV/c^2 obtained from MC, and use three–body phase space [1] to describe the background shape. Even though we exclude the high mass region to avoid the B_s contamination, there is still a small contribution in the region of interest. We obtained the ΔM shape from B_s contamination and fix the ΔM shape obtained from B_s MC simulation, and the yield to 3.3, scaled from the $B_s \to J/\psi\phi$ yield in data. An unbinned likelihood fit to the ΔM distribution, as shown in Fig. 5, returns a yield of 19 ± 6 events, a ΔM of $1046.7^{+2.9}_{-3.0}$ MeV/c^2, and a width of $15.3^{+10.4}_{-6.1}$ MeV/c^2.

We use the log-likelihood ratio of $-2\ln(\mathcal{L}_0/\mathcal{L}_{max})$ to determine the significance of the structure at the $J/\psi\phi$ threshold, where $\mathcal{L}_0$ and $\mathcal{L}_{max}$ are the likelihood values for the null hypothesis fit and signal hypothesis fit. Both fits use three–body phase space to describe the background. The $\sqrt{-2\ln(\mathcal{L}_0/\mathcal{L}_{max})}$ value obtained in data is 5.9. We

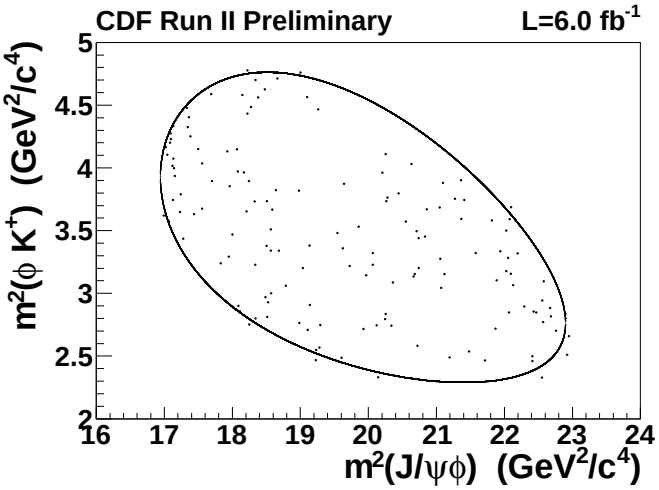

FIG. 3: The Dalitz plot of $m^2(\phi K^+)$ versus $m^2(J/\psi\phi)$ for events in the B^+ mass window in our data sample.

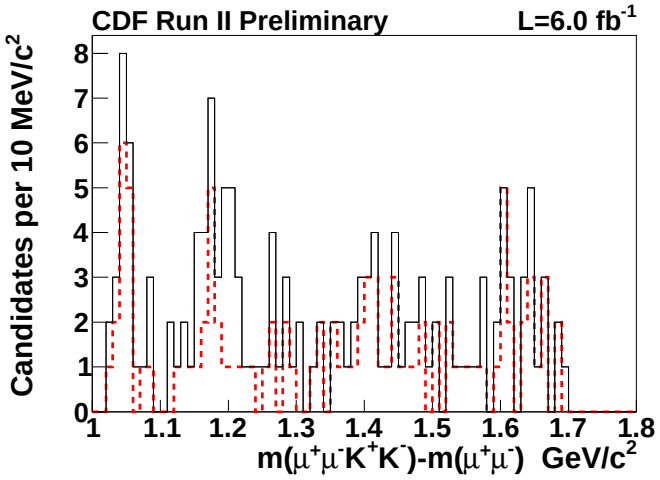

FIG. 4: The ΔM distribution in the B mass window for the data used in the current analysis (6.0 fb^{-1}) is shown as the black histogram, and the same distribution for the data in the previous analysis(2.7 fb^{-1} [12])is shown as the red dashed histogram.

use the simulation process described in Reference [12], based on a pure three–body phase space background shape, to determine the significance of the $Y(4140)$ structure. We performed a total of 84 million simulations and found 19 trials with a $-2\ln(\mathcal{L}_0/\mathcal{L}_{max})$ value greater than or equal to the value obtained in the data, as shown in Fig. 6. The resulting p-value is 2.3×10^{-7}, corresponding to a significance of greater than 5.0σ. We then fit to the tail of the $-2\ln(\mathcal{L}_0/\mathcal{L}_{max})$ distribution (from 2 to 50) obtained from simulation using a χ^2 probability density function [1] to get the χ^2 degree of freedom. The p-value by integrating the distribution from the observed $-2\ln(\mathcal{L}_0/\mathcal{L}_{max})$ value to infinity is 1.8×10^{-7}, which is consistent with the p-value obtained from counting. (We do not assume a flat background shape as before since it is unphysical and the events from the B sideband show no events in the region of interest.) This distribution is shown in Fig. 7.

The mass of this structure is $4143.4^{+2.9}_{-3.0}$ MeV/c^2 after including the world-average J/ψ mass. To study the systematic uncertainties of the mass, width and yield, we repeat the fit to the ΔM distribution while varying the background shapes, and separately switching to a non–relativistic BW for signal. The largest deviations from the nominal values are 0.6 MeV/c^2 for ΔM, 1.9 MeV/c^2 for the width, and 3 for the yield. Therefore we assign a systematic uncertainty of 0.6 MeV/c^2 to the mass, 1.9 MeV/c^2 to the width, and 3 for the yield. The relative efficiency between $B^+ \to Y(4140)K^+, Y(4140) \to J/\psi\phi$ and $B^+ \to J/\psi\phi K^+$ is 1.1 assuming $Y(4140)$ as an S-wave BW structure with mean and width values determined from the data, and three-body phase space kinematics for the $B^+ \to J/\psi\phi K^+$ decay. Systematic uncertainties in the branching fraction measurement include PID (16%) and signal modeling

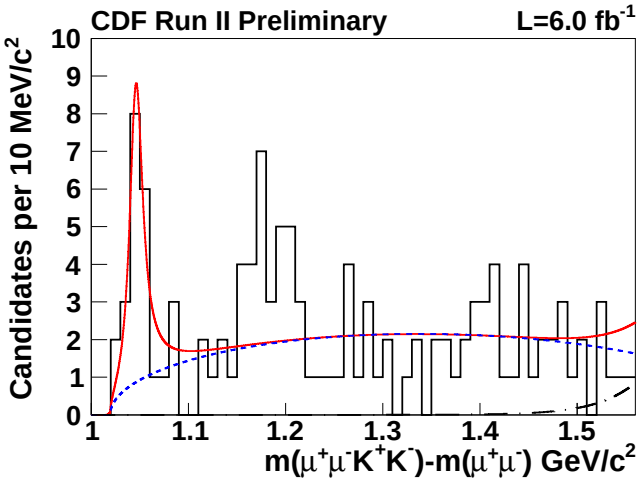

FIG. 5: The mass difference, ΔM, between $\mu^+\mu^-K^+K^-$ and $\mu^+\mu^-$, in the B^+ mass window is shown as a solid black histogram for the data. The dotted curve is the predicted three-body phase space background contribution, the dash-dotted curve is the predicted B_s contamination (fixed to 3.3), and the solid red curve is the total unbinned fit where the signal PDF is an S-wave Breit-Wigner convoluted with the resolution (1.7 MeV/c^2).

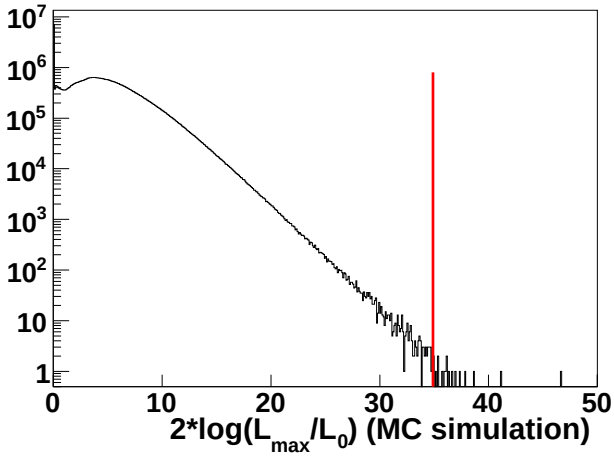

FIG. 6: Distribution of $-2\ln(\mathcal{L}_0/\mathcal{L}_{max})$ for 84 million simulation trials. The p-value obtained from counting is 2.3×10^{-7}, corresponding to a significance of greater than 5.0σ.

(16%). Thus the relative branching fraction between $B^+ \to Y(4140)K^+, Y(4140) \to J/\psi\phi$ and $B^+ \to J/\psi\phi K^+$, BF_{rel}, including systematics is $0.149 \pm 0.039(\text{stat}) \pm 0.024(\text{syst})$.

An excess above the three-body phase space background shape appears at approximately 1.18 GeV/c^2 in Fig. 1 (b). Since the significance of $Y(4140)$ is greater than 5σ, we fit to the data assuming two structures at ΔM of 1.05 and 1.18 GeV/c^2 as shown in Fig. 8. The fit to the data with the same requirements as in the previous paper [12] returns a yield of 20 ± 5 events, a ΔM of $1046.7^{+2.8}_{-2.9}$ MeV/c^2 , and a width of $15.0^{+8.5}_{-5.6}$ MeV/c^2 for the $Y(4140)$, which are consistent with the values returned from a $Y(4140)$-only signal fit. The fit returns a yield of 22 ± 8 events, a ΔM of $1177.7^{+8.4}_{-6.7}$ MeV/c^2 , and a width of $32.3^{+21.9}_{-15.3}$ MeV/c^2 for the structure around ΔM of 1.18 GeV/c^2 . The $\sqrt{-2\ln(\mathcal{L}_0/\mathcal{L}_{max})}$ for the second structure is 4.1, where $\mathcal{L}_0$ and $\mathcal{L}_{max}$ are the likelihood values for the null hypothesis fit assuming the $Y(4140)$-only and signal hypothesis fit assuming the $Y(4140)$ and a structure around ΔM of approximately 1.18 GeV/c^2 . The p-value determined by a similar simulation is 1.1×10^{-3}, as shown in Fig. 9 which corresponds to a significance of 3.1σ.

In summary, the increased $B^+ \to J/\psi\phi K^+$ sample at CDF enables us to further investigate the $Y(4140)$ structure and we find that its mass and width are consistent with the previous report [12] with a significance greater than 5σ. Assuming an S-wave relativistic BW, the mass and width of this structure, including systematic uncertainties,

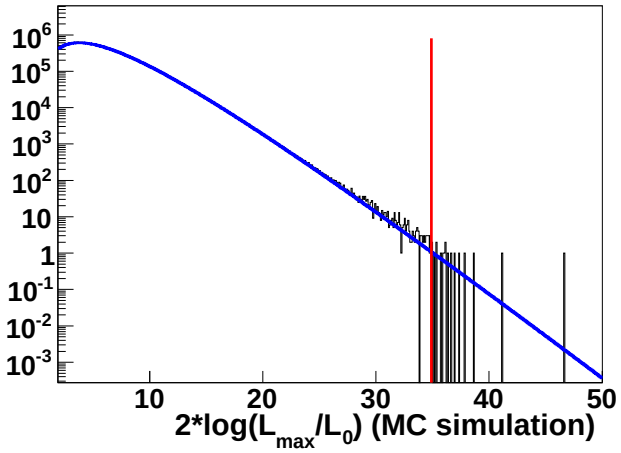

FIG. 7: Distribution of $-2\ln(\mathcal{L}_0/\mathcal{L}_{max})$ for 84 million simulation trials. The p-value obtained from integrating the tail of the distribution is 1.8×10^{-7}.

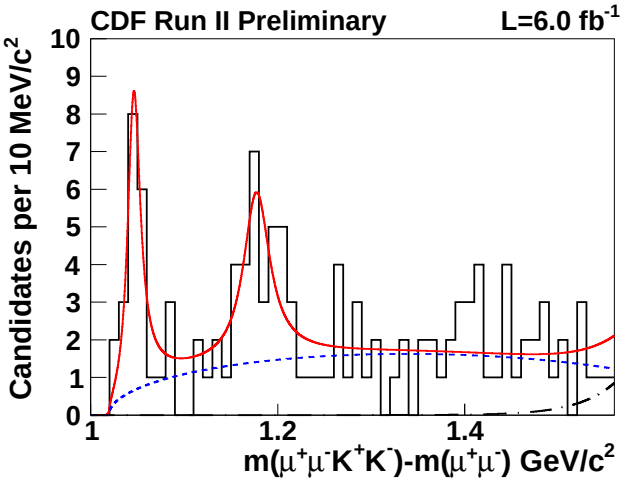

FIG. 8: The mass difference, ΔM, between $\mu^+\mu^-K^+K^-$ and $\mu^+\mu^-$, in the B^+ mass window. The dotted curve is the background contribution, the dash-dotted curve is the B_s contamination, and the red solid curve is the total unbinned fit assuming two structures. The shaded histogram is the events from B sideband.

are measured to be $4143.4^{+2.9}_{-3.0}(\text{stat}) \pm 0.6(\text{syst})$ MeV/c^2 and $15.3^{+10.4}_{-6.1}(\text{stat}) \pm 2.5(\text{syst})$ MeV/c^2, respectively. The relative branching fraction between $B^+ \to Y(4140)K^+, Y(4140) \to J/\psi\phi$ and $B^+ \to J/\psi\phi K^+$ including systematics, BF_{rel}, is $0.149 \pm 0.039(\text{stat}) \pm 0.024(\text{syst})$. We also find a hint of a possible second structure with a mass of $4274.4^{+8.4}_{-6.7}(\text{stat})$ MeV/c^2, a width of $32.3^{+21.9}_{-15.3}(\text{stat})$ MeV/c^2 and a yield of 22 ± 8. The significance of the second possible structure is estimated to be approximately 3.1σ.

[1] C. Amsler *et al.* (Particle Data Group), Phys. Lett. B **667**, 1 (2008).

[2] S.-K. Choi *et al.* (Belle Collaboration), Phys. Rev. Lett. **91**, 262001 (2003); D. Acosta *et al.* (CDF Collaboration), Phys. Rev. Lett. **93**, 072001 (2004); V. M. Abazov *et al.* (D0 Collaboration), Phys. Rev. Lett. **93**, 162002 (2004); B. Aubert *et al.* (*BABAR* Collaboration), Phys. Rev. D **71**, 071103(R) (2005).

[3] S.-K. Choi *et al.* (Belle Collaboration), Phys. Rev. Lett. **94**, 182002 (2005); B. Aubert *et al.* (*BABAR* Collaboration), Phys. Rev. Lett. **101**, 082001 (2008).

[4] B. Aubert *et al.* (*BABAR* Collaboration), Phys. Rev. Lett. **95**, 142001 (2005).

[5] B. Aubert *et al.* (*BABAR* Collaboration), Phys. Rev. Lett. **98**, 212001 (2007); X. L. Wang *et al.* (Belle Collaboration),

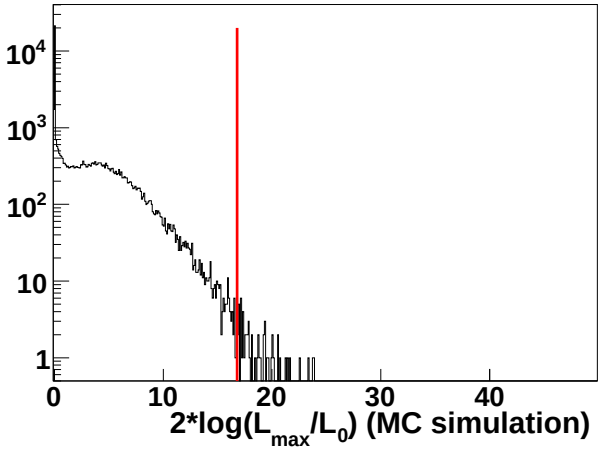

FIG. 9: Distribution of $-2\ln(\mathcal{L}_0/\mathcal{L}_{max})$ for simulation trials. The p-value obtained from counting is 1.1×10^{-3}, corresponding to a significance of 3.1σ.

Phys. Rev. Lett. **99**, 142002 (2007); S.-K. Choi *et al.* (Belle Collaboration), Phys. Rev. Lett. **100**, 142001 (2008); R. Mizuk *et al.* (Belle Collaboration), Phys. Rev. D **78**, 072004 (2008); P. Pakhlov *et al.* (Belle Collaboration), Phys. Rev. Lett. **100**, 202001 (2008).

[6] E. Eichten, K. Lane, and C. Quigg, Phys. Rev. D **69**, 094019 (2004); E. Eichten, S. Godfrey, H. Mahlke, and J. Rosner, Rev. Mod. Phys. **80**, 1161 (2008).

[7] S. L. Zhu, Phys. Lett. B **625**, 212 (2005); F. Close and P. Page, Phys. Lett. B **628**, 215 (2005).

[8] E. S. Swanson, Phys. Lett. B **588**, 189 (2004).

[9] L. Maiani, F. Piccinini, A. D. Polosa, and V. Riquer, Phys. Rev. D **72**, 031502(R) (2005); D. Ebert, R. N. Faustov, and V. O. Galkin, Eur. Phys. J. C **58**, 399 (2008).

[10] Yu. S. Kalashnikova and A. V. Nefediev, Phys. Rev. D **77**, 054025 (2008); E. J. Eichten, Private communication; P. Hasenfratz, R. R. Horgan, J. Kuti, and J. -M. Richard, Phys. Lett. B **95**, 299 (1980); S. Perantonis and C. Michael, Nucl. Phys. **B347**, 854 (1990); C. Bernard *et al.*, Phys. Rev. D **56**, 7039 (1997); X. Liao and T. Manke, arXiv:hep-lat/0210030.

[11] N. V. Drenska, R. Faccini, and A. D. Polosa, arXiv:hep-ph/0902.2803v1.

[12] T. Aaltonen *et al.* (CDF Collaboration), Phys. Rev. Lett. **102**, 242002 (2009) .

[13] F. E. Close *et al.*, Phys. Rev. D **57**, 5653 (1998); F. E. Close and S. Godfrey, Phys. Lett. B **574** 210 (2003).

[14] X. Liu and S. Zhu, arXiv:hep-ph/0903.2529.

[15] D. Acosta *et al.* (CDF Collaboration), Phys. Rev. D **71**, 032001 (2005); A. Abulencia *et al.* (CDF Collaboration), Phys. Rev. Lett. **97**, 242003 (2006).

[16] We use a coordinate system in which the proton beam direction is defined as the z axis. The angle θ is the usual polar angle. We define the pseudorapidity as $\eta \equiv -\ln(\tan\frac{\theta}{2})$. The transverse momentum is defined as $p_T = p\sin\theta$, where p is the momentum measured in the tracking system.

[17] T. Aaltonen *et al.* (CDF Collaboration), Phys. Rev. Lett. **100**, 101802 (2008).

[18] B. Aubert *et al.* (*BABAR* Collaboration), Phys. Rev. Lett. **97**, 112002 (2006); B. Aubert *et al.* (*BABAR* Collaboration), Phys. Rev. D **74**, 111103 (2006).

[19] M. Pivk and F. R. Le Diberder, Nucl. Instrum. Meth. A **555**, 356 (2005).

[20] A. Abulencia *et al.* (CDF Collaboration), Phys. Rev. Lett. **97**, 242003 (2006).

[21] A. Abulencia *et al.* (CDF Collaboration), Phys. Rev. Lett. **96**, 082002 (2006); T. Aaltonen *et al.* (CDF Collaboration), Phys. Rev. Lett. **100** 182002 (2008).

[22] $\frac{dN}{dm} \propto \frac{m\Gamma(m)}{(m^2-m_0^2)^2+m_0^2\Gamma^2(m)}$, where $\Gamma(m) = \Gamma_0 \frac{q}{q_0}\frac{m_0}{m}$, and the 0 subscript indicates the value at the peak mass.

[23] B. Aubert *et al.* (*BABAR* Collaboration), Phys. Rev. D **78**, 071103 (2008).

[24] T. Armstrong *et al.*, Nucl. Phys. **B221**, 1 (1983).